Microscopic analysis of complete ^{90}Zr(p,n) spectra including the Δ isobar effect

F. Osterfeld, D. Cha, and J. Speth*
Institut für Kernphysik, Kernforschungsanlage Jülich, D-5170 Jülich, Federal Republic of Germany
(Received 28 August 1984)

A microscopic analysis of the complete forward angle spectra of the ^{90}Zr(p,n) reaction is presented for an incident energy of 200 MeV. It is shown that the whole spectra up to an excitation energy of $E_x = 70$ MeV are the result of correlated one-particle—one-hole (1p1h) spin-isospin transitions only. The spectra reflect, therefore, the linear spin-isospin response of the target nucleus to the probing (p,n) field. Two different cross section calculations are performed: one with usual random phase approximation wave functions and one with generalized random phase approximation wave functions which include Δ isobar degrees of freedom explicitly. We find that the theoretical cross sections calculated with random phase approximation wave functions, which provide the lower limit of spin-isospin strength, describe the data rather well at all scattering angles, while the random phase approximation + Δ cross sections underestimate the data at forward angles. In this connection we discuss the quenching of the spin-isospin strength in detail.

I. INTRODUCTION

The recent discovery of the giant Gamow-Teller resonances (GTR) by intermediate energy (p,n) reactions[1–5] has led to a major breakthrough in our understanding of spin-isospin correlations in nuclei. In particular, the zero degree (p,n) spectra are dominated by one prominent peak which is interpreted as the GTR with quantum numbers $J^\pi = 1^+$, $L = 0$, $S = 1$, $T = 1$. This collective mode which is the spin-isospin nuclear sound was already predicted by Ikeda, Fujii, and Fujita[6] as early as 1963. The GTR appears energetically in the continuum region of the nuclear excitation spectrum and possesses a width of about 6 MeV. While its excitation energy is well reproduced by the common random phase approximation (RPA),[7] there is much less Gamow-Teller (GT) strength observed in the (p,n) experiments[8] than predicted by the RPA. Three physically different mechanisms have been discussed to explain this so-called quenching of the total GT strength. The first is that Δ(1232)-isobar—nucleon-hole (ΔN^{-1}) states couple into the proton-particle—neutron-hole (pn^{-1}) GT states and remove strength from the low-lying excitation spectrum.[9–12] Here the internal degrees of freedom of the nucleon, specifically the Δ, are made responsible for the quenching of the GT strength. The second mechanism is ordinary nuclear configuration mixing,[12–14] where energetically high-lying two-particle—two-hole (2p2h) states mix with the low-lying one-particle—one-hole (1p1h) GT state and shift GT strength into the energy region far beyond the GTR. The third possibility,[15,16] closely connected with the second mechanism, is that a large fraction of GT strength is actually located in the physical background below and beyond the giant GT state and is therefore escaping experimental detection. The most exciting quenching mechanism is the one which involves the Δ isobar. Here the collective GT mode is coupled with an internal nucleon excitation which can be thought of as a spin-isospin flip transition of a quark in the nucleon. In how far this mechanism is effective is not easy to decide, especially in view of the other possible quenching mechanisms. The answer to this question is, however, of fundamental importance for our understanding of nuclear spin-isospin excitations and, in particular, also for our understanding of the role of the Δ in nuclei.

In this paper, we attack this question by starting out from the measured (p,n) spectra at different scattering angles θ. We develop a microscopic model which permits us to calculate the spectra at all scattering angles in a consistent way. The model wave functions for the nuclear excited states are generated from microscopic RPA calculations. Two different configuration spaces are used: in the first one we consider the nucleus to consist of nucleons only, whereas in the second one Δ isobars are also included explicitly. Using these two different sets of wave functions we analyze ^{90}Zr(p,n) spectra[5] at an incident energy of 200 MeV. We show that essentially all the measured cross sections up to an excitation energy of $E_x = 70$ MeV are produced by 1p1h spin-isospin excitations. Our calculations describe not only the peaks in the spectra but also the continuous parts which are usually termed *background*. We decompose the spectra into various multipoles and determine the strength distribution functions of the various spin-isospin modes such as the GT ($L = 0, S = 1, T = 1$), the spin flip dipole ($L = 1, S = 1, T = 1$), and the spin flip quadrupole ($L = 2, S = 1, T = 1$) modes. The $L = 1$ resonance appears energetically at roughly 10 MeV above the GTR and possesses a width of about 10 MeV. It has been interpreted as the envelope of three collective states with spin parity $J^\pi = 0^-$, 1^-, and 2^-.[17] The $L = 2$ resonance is a $2\hbar\omega$ mode and includes states with spin parity $J^\pi = 1^+$, 2^+, and 3^+.

Since we analyze the experimental spectra in the whole excitation range from $E_x = 0$ to 70 MeV and in the whole angle range from 0 to 18.7 deg, we are in a good position to make reliable statements about the total amount of spin-isospin transition strength observed in the (p,n) reac-

tions and about the question of whether or not there is need for quenching of GT strength (or generally spin-isospin strength) due to Δ isobars. By considering the whole spectra we exclude two major uncertainties which usually occur in the analysis of the data. First, we have no background problem because we calculate the whole spectra. Second, uncertainties in the strength extraction which are produced by the 2p2h nuclear configuration mixing mechanism are minimized because we investigate the spectra up to very high excitation energies. If there should exist a strong shift of 1p1h transition strength to high excitation energies (due to the 2p2h configuration mixing effect), we will see this directly from the analysis of the data.

Looking to the spectra as a whole means looking to total sum rule strengths. In the case of the GT transitions we have a very general model independent sum rule.[18] This sum rule connects the neutron excess $(N-Z)$ of a nucleus with the difference between the $\sigma\tau_-$ strength S_{β_-} measured in β_- decay and the $\sigma\tau_+$ strength S_{β_+} measured in β_+ decay in the following way:

$$S_{\beta_-}=3(N-Z)+S_{\beta_+} . \tag{1}$$

Here, S_{β_-} and S_{β_+} are defined by

$$S_{\beta_\pm}=\sum_f \sum_\mu \left|\left\langle f\left|\sum_{k=1}^{A}\sigma_\mu(k)\tau_\pm(k)\right|i\right\rangle\right|^2 , \tag{2}$$

where $|i\rangle$ and $|f\rangle$ denote the initial and final nucleus states, respectively. We use this sum rule in order to give a lower limit for the amount of S_{β_-} strength observed in the (p,n) reactions. From the sum rule itself one obtains the lower limit for S_{β_-} by putting $S_{\beta_+}=0$, i.e., $S_{\beta_-}=3(N-Z)$. This condition is approximately fulfilled for nuclei with a large neutron excess. In this case the S_{β_+} strength is small because all states for transferring a proton into a neutron within the same major shell are Pauli blocked. For example, if we assume an uncorrelated shell model ground state for ^{90}Zr, then the S_{β_+} strength is zero due to the Pauli blocking. The 2p2h admixtures into the ground state, however, change this result and give rise to S_{β_+} strength because the sharp proton and neutron Fermi surfaces are smeared out. Therefore, also the S_{β_-} strength is changed and becomes now larger than the $3(N-Z)$ limit. In Ref. 14, this effect of ground state correlations was estimated for ^{90}Zr with the result that the S_{β_-} was increased by $\sim 20\%$ as compared with the $3(N-Z)$ value. A similar effect might also be expected for states with higher multipolarities such as the $L=1$ and $L=2$ resonances. In our analysis of the (p,n) spectra, ground state correlations of the 2p2h-type are not included. Therefore, all our theoretical cross sections are lower limits and include only $\sigma\tau_-$ strength in the GT case given by the lower sum rule limit $S_{\beta_-}=3(N-Z)$.

In Sec. II, we briefly describe the model assumptions made in the calculations and give details about the nuclear structure and reaction calculations. In Sec. III we present the results of our microscopic analyses of the ^{90}Zr(p,n) spectra. In Sec. IV, we summarize the main conclusions of this work.

II. THE MODEL

A. The model assumptions

The basic model assumption in our analysis of the data is that for (p,p′) and (p,n) reactions at high incident energies ($E_p > 100$ MeV) the cross section at forward angles is dominated by direct processes as long as the excitation energy is less than half the beam energy. This assumption is supported by both experiment and theory. The 0° cross sections of the 200 MeV (p,n) data of Gaarde *et al.*,[5] for instance, show a characteristic falling off with increasing excitation energy (see also Fig. 2). Large contributions of multistep processes, however, should instead lead to a *rise* in cross sections with increasing excitation energy due to the greater number of intermediate states available for higher energy losses. Calculations of multistep reaction cross sections by Chiang and Hüfner[19] show that the forward angle cross sections in high energy (p,p′) reactions are largely due to one-step processes. Also the microscopic (p,n) background calculations by one of the present authors[15] showed that this assumption is indeed correct. Therefore, we may assume that the 200 MeV ^{90}Zr(p,n) spectrum at forward angles is a simple superposition of cross sections of inelastic excitations to bound, quasi-bound, and continuum states.

Since the impulse approximation[20,21] was shown to be very accurate at intermediate energies, we shall approximate the effective projectile-target nucleon interaction by the free nucleon-nucleon (NN) t matrix in the parametrization of Love and Franey.[21] The only nuclear states which are then contributing to the (p,n) spectrum are the spin flip ($S=1, T=1$) states. This argument is based on the fact that the $\sigma\tau$ part of the free NN t matrix[21] which excites the spin flip states is nearly energy independent, while the τ part which excites the nonspin flip states gets strongly reduced at $E \geq 100$ MeV. The cross sections to the latter states are then much smaller in comparison to those of the former. For this reason we neglect cross sections to nonspin flip states in our analysis of the (p,n) spectra except that of the isobaric analog state (IAS). From the spin flip states we include all states with multipolarities $L=0$–4 ($J^\pi=0^-,1^+,1^-,2^+,2^-,3^+,3^-,4^-,4^+,5^+$). The wave functions of most of these states ($J^\pi=0^-,1^-,2^-,1^+,2^+,3^+$) are based on the RPA, while the rest of the states are still treated within the unperturbed 1p1h doorway model of Refs. 15 and 16.

B. The structure calculations

The wave functions for the nuclear excited states were calculated within the RPA. The RPA calculations were performed in the same way as described in Ref. 10. For the residual particle-hole (ph) interaction we used a realistic interaction which includes the one-pion (π) and one-rho (ρ) exchange potentials in the $\sigma\tau$ channel explicitly. The effects of the other mesons are summarized in a two-body correlation function and an additional zero-range

term. The explicit form of the ph interaction in momentum space is then given by:

$$V_{\rm ph}(\mathbf{q})=\int g(\mathbf{k}-\mathbf{q})[V_\pi(\mathbf{k})+V_\rho(\mathbf{k})]\frac{d^3k}{(2\pi)^3}$$
$$+\delta g'_0 C_0 \boldsymbol{\sigma}_i\cdot\boldsymbol{\sigma}_2\boldsymbol{\tau}_1\cdot\boldsymbol{\tau}_2\ , \tag{3a}$$

$$g(\mathbf{q})=(2\pi)^3\delta(\mathbf{q})-\frac{2\pi^2}{q_c^2}\delta(|\mathbf{q}|-q_c)\ ,\quad q_c=3.93\ \text{fm}^{-1}\ , \tag{3b}$$

$$V_\pi(\mathbf{q})=-\frac{f_\pi^2}{m_\pi^2}\left[\frac{\Lambda_\pi^2-m_\pi^2}{\Lambda_\pi^2+q^2}\right]^2\frac{\boldsymbol{\sigma}_1\cdot\mathbf{q}\boldsymbol{\sigma}_2\cdot\mathbf{q}}{m_\pi^2+q^2}\boldsymbol{\tau}_1\cdot\boldsymbol{\tau}_2\ , \tag{3c}$$

$$V_\rho(\mathbf{q})=-\frac{f_\rho^2}{m_\rho^2}\left[\frac{\Lambda_\rho^2-m_\rho^2}{\Lambda_\rho^2+q^2}\right]^2\frac{\boldsymbol{\sigma}_1\times\mathbf{q}\boldsymbol{\sigma}_2\times\mathbf{q}}{m_\rho^2+q^2}\boldsymbol{\tau}_1\cdot\boldsymbol{\tau}_2\ , \tag{3d}$$

$$f_\pi^2=0.081\ ,\quad m_\pi=0.699\ \text{fm}^{-1}\ ,$$
$$\Lambda_\pi=6\ \text{fm}^{-1}\ ,\quad f_\rho^2=4.86\ ,$$
$$m_\rho=3.9\ \text{fm}^{-1}\ ,\quad \Lambda_\rho=10\ \text{fm}^{-1}\ , \tag{3e}$$
$$C_0=302\ \text{MeV fm}^3\ ,\quad \delta g'_0=0.5\ .$$

The interaction between nucleons and isobars was obtained from Eq. (3) by replacing the spin and isospin operators σ and τ by the transition operators **S** and **T**, respectively, and by assuming the Chew-Low value $f_{\pi N\Delta}=2f_{\pi NN}$ and correspondingly $f_{\rho N\Delta}=2f_{\rho NN}$ (Ref. 22) for the nucleon-isobar coupling constant. Both the direct and exchange terms of the finite range parts of the ph interaction were taken into account in the nucleonic and the Δ isobar sectors. A large model space was used for the RPA calculations which included all $\leq 3\hbar\omega$ ph excitations for the pn^{-1} configurations and all isobar orbits from $1s$ to $1j$ for the ΔN^{-1} configurations. The single particle energies and single particle wave functions were generated from a Woods-Saxon potential which was chosen to reproduce the known experimental single particle energies. The generalized RPA wave functions including ΔN^{-1} configurations are then given by

$$\Psi^J=\left[\sum_{\rm ph}\chi^J(\text{ph})a_{\rm p}^\dagger a_{\rm h}+\sum_{\Delta h}\chi^J(\Delta\text{h})a_\Delta^\dagger a_{\rm h}\right]|\,\text{g.s.}\rangle\ , \tag{4}$$

where $\chi^J(\text{ph})$ and $\chi^J(\Delta\text{h})$ are the RPA transition amplitudes of the $|NN^{-1}\rangle$ and $|\Delta N^{-1}\rangle$ configurations, respectively.

C. The reaction calculations

From the wave functions of Eq. (4), we calculate the (p,n) cross sections with the fast-speed DWBA code FROST-MARS which includes knock-out exchange amplitudes exactly.[23] Also for the Δ excitations we calculate both the direct and the knock-out exchange amplitudes. For the projectile-isobar interaction (see Fig. 1) we simply used the one-pion and one-rho exchange potentials in which we replaced the spin (σ) and isospin (τ) operators by the transition operators **S** and **T**. Again we assumed

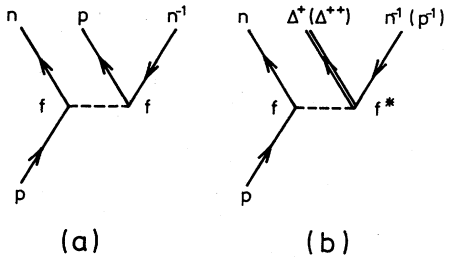

FIG. 1. Graphical representation of reaction processes included in the distorted-wave impulse approximation calculations. Only direct graphs are shown. For the effective projectile-target nucleon interaction the parametrization of Love and Franey (Ref. 21) is used (see the text) and for the projectile-isobar coupling the $\pi+\rho$ potential with the coupling constant $f^*=2f$ (Chew-Low value Ref. 22) has been taken.

$f_{\pi N\Delta}=2f_{\pi NN}$ and $f_{\rho N\Delta}=2f_{\rho NN}$ for the nucleon-isobar coupling constant. A similar projectile-isobar interaction was already successfully used in the analysis of 160 MeV ^{48}Ca(p,n) data in Ref. 11.

D. Normalization to β decay

The effective projectile-target nucleon interaction has to be calibrated before it can be used in the reaction calculations in order to guarantee a force independent analysis of the spectra. In our calibration procedure we proceed as follows: First we make use of the fact that the zero degree (p,n) cross section for $L=0, S=1, 1^+$ transitions is proportional to the GT strength of these states. This follows simply from the low momentum transfer (q) limit of the zero degree GT cross section which in the impulse approximation can be written as[3]

$$\frac{d\sigma}{d\Omega}(q\sim 0)=\left[\frac{\mu}{\pi\hbar}\right]^2\frac{k_f}{k_i}N_{\sigma\tau}\,|\,\mathcal{J}_{\sigma\tau}^{\rm NN}\,|^2 B(\text{GT})\ , \tag{5}$$

where k_i and k_f denote the initial and final projectile wave numbers, respectively, and μ denotes the reduced mass. $N_{\sigma\tau}$ is the distortion factor by which the cross section is reduced due to the absorption of the incoming and outgoing waves, and $\mathcal{J}_{\sigma\tau}$ is the volume integral of the effective projectile-target nucleon interaction which induces the $\sigma\tau$ transitions. The B(GT) value for the nuclear transition $i\rightarrow f$ is defined as

$$B(\text{GT})=\sum_\mu\left|\left\langle f\left|\sum_{k=1}^A\sigma_\mu(k)\tau(k)\right|i\right\rangle\right|^2\ . \tag{6}$$

By selecting now a GT transition with a known B(GT) value and known experimental zero degree (p,n) cross section, we can fix the volume integral $\mathcal{J}_{\sigma\tau}$ in Eq. (5) or, equivalently, the effective interaction $V_{\sigma\tau}(q=0)$ at zero momentum transfer q. A good candidate for such a calibration procedure is the transition

$$^{42}\text{Ca}(0^+)\rightarrow{}^{42}\text{Sc}(1^+\ ,\ E_x=0.61\ \text{MeV})$$

which possesses a B(GT) value of 2.57 ($\log ft=3.17$) and a large 0° (p,n) cross section. The same transition is also

used by the experimentalists[5,8] to normalize measured zero degree (p,n) cross sections to β decay. Since the β decay determines the B(GT) value in a model independent way we may perform the 0° (p,n) cross section calculation with any set of initial and final nucleus wave functions which reproduce the measured B(GT) value. Accidentally, for the ^{42}Ca(0^+)$\rightarrow$^{42}Sc(1^+) transition, a simple $[f_{7/2}]^2$ wave function for the 0^+ state in ^{42}Ca and the 1^+ state in ^{42}Sc already fulfills this condition and gives almost exactly the B(GT) value of 2.57. Using these wave functions and using the 210 MeV t matrix of Love and Franey[21] for the effective projectile-target nucleon interaction we calculate a zero degree (p,n) cross section of 13.4 mb for the

$$^{42}\mathrm{Ca(p,n)}^{42}\mathrm{Sc}(1^+ , E_x = 0.61\ \mathrm{MeV})$$

reaction at 200 MeV incident energy. The experimental cross section amounts to 15.5 mb (Ref. 24) so that we have to renormalize the theoretical cross section by a factor of 15.5/13.4=1.16. We remark that this renormalization not necessarily implies a renormalization of the Love-Franey interaction.[21] From Eq. (5) it is evident that the distortion factor $N_{\sigma\tau}$ could also be responsible for this. The latter depends on the optical parameters used. We remark further that by the preceding calibration procedure we only calibrate the absolute magnitude of the effective interaction at $q=0$, but not yet its q dependence. The latter can be checked, however, by analyzing angular distributions of inelastic or charge exchange reactions to states with known nuclear structure. The q dependence of the $\sigma\sigma\tau\tau$ central *and* tensor components of the Love-Franey interaction[21] has been tested, for instance in Ref. 11, and found to be essentially in agreement with experiment.

The calibration procedure has to be modified somewhat if the nuclear wave functions include ΔN^{-1} components. Let us assume that the final nuclear wave function is given by

$$|\Psi_f\rangle = a\,|\mathrm{NN}^{-1}\rangle - b\,|\Delta\mathrm{N}^{-1}\rangle\ , \tag{7}$$

where $|\mathrm{NN}^{-1}\rangle$ and $|\Delta\mathrm{N}^{-1}\rangle$ stand schematically for the nuclear part and the Δ part of the wave function, respectively. In this case we have to replace the quantity $|\mathcal{J}_{\sigma\tau}^{\mathrm{NN}}|^2 B(\mathrm{GT})$ in Eq. (5) by

$$|\mathcal{J}_{\sigma\tau}^{\mathrm{NN}}|^2 B(\mathrm{GT}) \rightarrow (\mathcal{J}_{\sigma\tau}^{\mathrm{NN}} a\langle \mathrm{NN}^{-1}|\sigma\tau|0\rangle - \mathcal{J}_{\sigma\tau}^{\mathrm{N\Delta}} b\langle \Delta\mathrm{N}^{-1}|ST|0\rangle)^2\ , \tag{8}$$

where $\mathcal{J}_{\sigma\tau}^{\mathrm{N\Delta}}$ denotes the volume integral of the effective projectile-Δ isobar interaction. The B(GT) value is now defined by

$$B(\mathrm{GT}) = \left[a\langle \mathrm{NN}^{-1}|\sigma\tau|0\rangle - \frac{g_A^*}{g_A} b\langle \Delta\mathrm{N}^{-1}|ST|0\rangle\right]^2 , \tag{9}$$

with g_A^*/g_A being the ratio of the axial vector coupling constants for the nuclear (g_A) and Δ-isobar (g_A^*) sector.

Now, we are in the situation that we have to fix two independent quantities with our calibration procedure, namely $\mathcal{J}_{\sigma\tau}^{\mathrm{NN}}$ and $\mathcal{J}_{\sigma\tau}^{\mathrm{N\Delta}}$. But, on the other hand, we have also two known quantities, the measured B(GT) value and the measured 0° (p,n) cross section. Let us suppose that Δ isobars quench the total GT strength to a certain amount. Then also the transition ^{42}Ca(0^+)$\rightarrow$^{42}Sc(1^+) should suffer from this quenching. Therefore, the ^{42}Ca(p,n)^{42}Sc(1^+) transition density has to contain ΔN^{-1} components, the admixture of which is determined by the mixing coefficient b in Eq. (7). The magnitude of b depends sensitively on the strength of the ΔN^{-1} interaction used in the nuclear structure calculations. [See Eq. (3).] By appropriate adjustment of the force parameters of this interaction one always can produce a wave function with ΔN^{-1} components which fits the measured B(GT) value, in particular also for ^{42}Ca$\rightarrow$^{42}Sc. The essential point for us is that with the same wave function we also have to reproduce the measured zero degree

$$^{42}\mathrm{Ca(p,n)}^{42}\mathrm{Sc}(1^+ , E_x = 0.61\ \mathrm{MeV})$$

cross section. This we achieve by varying independently the volume integrals $\mathcal{J}_{\sigma\tau}^{\mathrm{NN}}$ and $\mathcal{J}_{\sigma\tau}^{\mathrm{N\Delta}}$. We find numerically only two sets of the volume integrals which satisfy simultaneously Eqs. (5) and (9), namely $\mathcal{J}_{\sigma\tau}^{\mathrm{N\Delta}}=0$ and

$$|\mathcal{J}_{\sigma\tau}^{\mathrm{N\Delta}}/\mathcal{J}_{\sigma\tau}^{\mathrm{NN}}| = g_A^*/g_A\ .$$

If the first set, $\mathcal{J}_{\sigma\tau}^{\mathrm{N\Delta}}=0$, would be valid, this would mean that the (p,n) probe would be "blind" for Δ's in nuclei. This is certainly not the case and therefore the second set

$$|\mathcal{J}_{\sigma\tau}^{\mathrm{N\Delta}}/\mathcal{J}_{\sigma\tau}^{\mathrm{NN}}| = g_A^*/g_A$$

is the correct one. This result is very important since it shows that the (p,n) probe at high incident energies sees Δ's in nuclei in the same way as the weak interaction in β decay. One can also say that the (p,n) reaction at zero degrees and high incident energies really measures GT strength. This has the further important consequence that from a careful study of (p,n) and (n,p) cross sections taken at the same incident energy one can test the Ikeda sum rule.[18]

Using the calibrated effective interaction, we can now go and analyze (p,n) spectra taken for other target nuclei. The only uncertainty in going from ^{42}Ca to another target nucleus is the distortion factor $N_{\sigma\tau}$ which changes for different target nuclei due to the different distortions. It turns out, however, that in going from ^{42}Ca to ^{90}Zr, for instance, the uncertainty is not larger than 10%. We checked this point by testing various sets of optical potential parameters,[25–27] including those of wine bottle shape.[27] After all we decided to use the global parameter set of Nadasen *et al.*[25] which is given as a function of the incident energy E and the target mass number A. This choice gives us the possibility to employ optical parameters of the same potential family for different target nu-

clei. We want to point out, however, that at 200 MeV incident energy these parameters lead to a 10% larger GT cross section in ^{90}Zr(p,n) than those determined from 200 MeV ^{90}Zr(p,p) elastic scattering data.[26] Therefore, all our conclusions presented in Sec. III might include such an uncertainty. Unfortunately there exist no experimentally determined optical model parameters for ^{42}Ca which would help to rule out this uncertainty. We also mention that there exists another uncertainty of the order of 10% which is connected with the normalization of the ^{90}Zr(p,n) data relative to the ^{42}Ca(p,n) data.[24]

III. RESULTS AND DISCUSSIONS

A. The 0° spectrum and the GT resonances

In the microscopic model already described we have calculated energy spectra at various scattering angles for the reaction ^{90}Zr(p,n) at 200 MeV incident energy. In Fig. 2 we show the results for the 0° and 4.5° spectra. The 0° spectrum in Fig. 2(a) is dominated by the GT 1^+ transitions. Two different theoretical spectra are compared to the data.[5] One is calculated with usual RPA wave functions (full curve) and the other with generalized RPA wave functions which include Δ isobar degrees of freedom (dashed curve). Both spectra are incoherent sums of cross sections with multipolarities $L=0$ through $L=4$ ($J^\pi=0^+,0^-,1^+,1^-,2^+,2^-,3^+,3^-,4^-,4^+,5^+$). From these states, the $0^-,1^-,2^-$ and $1^+,2^+,3^+$ states were calculated either with RPA or with RPA + Δ, while the $3^-,4^-,4^+,5^+$ states were treated within the unperturbed 1p1h doorway model of Ref. 15 which includes the nuclear continuum exactly. The RPA model space included all $3\hbar\omega$ excitations so that the RPA states extend in excitation energies up to a Q value of $Q=-40$ MeV. (Apart from the small proton-neutron mass difference $\Delta m=0.75$ MeV, the negative Q value is equal to the target excitation energy E_x: $E_x\sim -Q$). The cross section beyond $Q=-40$ MeV is mainly due to states with $E_x>3\hbar\omega$ which were again treated within the unperturbed 1p1h doorway model of Ref. 15.

The continuous spectra in Fig. 2 were obtained by folding the cross sections to the discrete states into a Breit-Wigner form with a width taken from experiment. The width was assumed to be 1 MeV for states with excitation energies E_x smaller or equal to the energy of the IAS, to be 6 MeV for the GT resonance and other states with $E_x\leq 15$ MeV, and to be 10 MeV for states with $E_x>15$ MeV. The width of the GT resonance had to be chosen asymmetrically in order to obtain a reasonably good fit to the experimental resonance shape. A total width of $\Gamma=6$ MeV was needed and split into two parts $\Gamma=\Gamma_{\text{left}}+\Gamma_{\text{right}}$ with $\Gamma_{\text{left}}=2$ MeV and $\Gamma_{\text{right}}=4$ MeV. Then these widths were used in an asymmetric Breit-Wigner form. For the

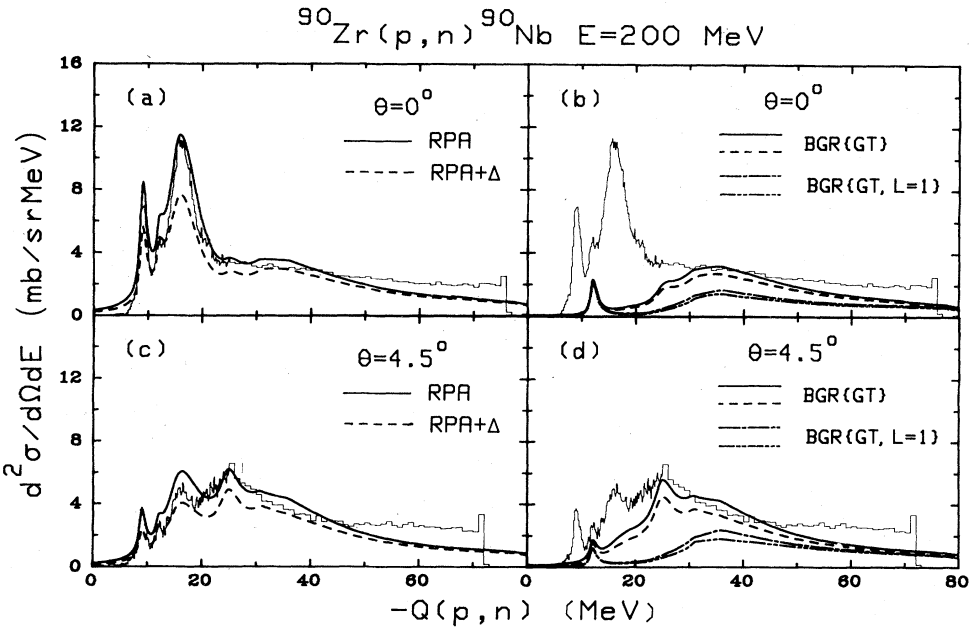

FIG. 2. Neutron spectra from the reaction ^{90}Zr(p,n)^{90}Nb at angles of $\theta=0°$ (a) and (b), and $\theta=4.5°$ (c) and (d). The data (thin full line) were taken from Ref. 5. The complete theoretical spectra in (a) and (c) were calculated either with usual RPA wave functions (thick full line) or with generalized RPA + Δ wave functions (dashed line). In the latter case the Δ isobar admixtures were adjusted such that the total GT strength is quenched by 30% (see the text). (b) and (d) show *backgrounds* (BGR) with respect to the GT resonance alone (BGR GT) and with respect to the GT *and* $L=1$ resonance (BGR GT, $L=1$). The full and the long-short-dashed lines represent the result obtained with RPA, and the dashed and the long-short-short-dashed lines represent the one obtained with RPA + Δ. By subtracting BGR GT, $L=1$ from BGR GT one obtains the strength distribution of the $1\hbar\omega$, $L=1$ resonance. In the energy range -20 MeV $\geq Q\geq -60$ MeV BGR GT, $L=1$ essentially coincides with the strength distribution of the $2\hbar\omega$, $J^\pi=1^+,2^+,3^+$ resonance.

states with $E_x > 15$ MeV, we employed the widths $\Gamma_{\text{left}} = 2$ MeV and $\Gamma_{\text{right}} = 8$ MeV, respectively.

By applying the described folding procedure to our cross section calculations we effectively simulate the damping (spreading) of the 1p1h RPA doorway states due to their coupling to 2p2h and more complicated configurations. When we spread the strength we have to take care of the fact that the (p,n) probe sees the shifted strength in a different way than the unshifted one. This is due to the Q-value dependence [or, equivalently, due to the momentum transfer (q) dependence] of the hadronic transition operator.[28] This effect we have taken into account in our calculations by introducing relative distortion factors defined by

$$\mathcal{D}(Q_0+\Delta Q,\theta,J) \equiv [d\sigma/d\Omega(Q_0+\Delta Q,\theta,J)]/[d\sigma/d\Omega(Q_0,\theta,J)] \tag{10}$$

which we multiply onto the cross section distribution functions. The distortion factors $\mathcal{D}$ are depending on the spin J of the final nucleus state, the energy shift ΔQ (Q_0: energy of the state considered), and the scattering angle θ. For $\Delta Q = 0$, we have $\mathcal{D}(Q_0,\theta,J) = 1$. The behavior of $\mathcal{D}$ as a function of ΔQ at fixed scattering angle θ can be determined from the shape of the angular distribution of the state under consideration, because an increase in ΔQ is equivalent to an increase in the momentum transfer Δq. The momentum transfer, however, can be varied in two ways namely either by changing the Q value or (and) by changing the scattering angle θ. Therefore, an increase in Q can also be simulated by an increase in θ which means that the qualitative behavior of $\mathcal{D}$ can be directly read off from the shape of the angular distribution to the given final nucleus state. For the GT state at $\theta = 0°$, for instance, $\mathcal{D}$ is decreasing with increasing ΔQ since the GT angular distribution possesses a $L = 0$ shape where L denotes the orbital angular momentum transfer. For all other states with multipolarities $L > 0$, however, $\mathcal{D}$ is increasing with increasing ΔQ at $\theta = 0°$ which again follows from the shapes of angular distributions with $L > 0$. This means that by shifting GT strength to higher excitation energies the total GT cross section at $\theta = 0°$ is reduced, while by shifting 0^-, 1^-, and 2^- strength, for instance, the total cross section to these states is increased at $\theta = 0°$.

From Fig. 2(a), we see that the 0° spectrum calculated with RPA reproduces the shape of the experimental spectrum rather well, but that it slightly overestimates the data in the low excitation energy region, while it underestimates them in the high excitation energy region. In order to bring theory and experiment into agreement in the low excitation energy region, one apparently has to introduce a quenching mechanism which reduces the amount of GT strength in the Q-value range -8 MeV $\geq Q \geq -22$ MeV. Two different quenching mechanisms have been proposed. In the first case the ΔN^{-1} states couple into the low-lying GT states and move part of the strength[9–12] into the Δ resonance region. In the second case energetically high-lying 2p2h states mix into the 1p1h GT states and shift GT strength from the low (0 MeV $\geq Q \geq -20$ MeV) to the high (-20 MeV $\geq Q \geq -70$ MeV) excitation energy region. In the latter case the total GT cross section is spread out continuously over a large energy range so that some of the GT strength will escape experimental detection. Which of the two quenching mechanisms is now dominantly effective can only be determined by a careful analysis of the complete forward angle (p,n) spectra. We intend to present such an analysis in the following.

Let us first discuss the assumption that only the 2p2h effect is responsible for the quenching of the GT strength by shifting strength from the low to the high excitation energy region. This effect is to a large extent already included in our calculation since we folded the discrete RPA cross sections into an asymmetric strength distribution function of Breit-Wigner form. Note, however, that these strength distribution functions lead to much less shift (spreading) of strength than those obtained in microscopic 2p2h configuration mixing calculations.[14,29–32] The 2p2h strength distribution functions have a long high energy tail which falls off only gradually. To that respect we assume a *minimal* spreading of strength in our calculations. It is interesting to know up to which excitation energy the GT strength is extending under this assumption of minimal spreading. To show this we first determine the *background* with respect to the GT states in the measured spectra. The cross section area in the spectrum not described by the *background* calculations should then be GT strength. The result for the GT *background* of the 0° spectrum is shown in Fig. 2(b). The full curve represents the result obtained with RPA and the dashed curve the one obtained with RPA + Δ (*quenched background*). The peak at $Q = -12$ MeV is due to the IAS and all the rest of the background cross section up to $Q = -70$ MeV is mainly due to the $1\hbar\omega$ $L = 1$ and $2\hbar\omega$ $L = 2$ resonances whose angular distributions, although peaking at larger scattering angles [see Figs. 2(c) and 3], are extending forward to 0°. The full curve in Fig. 2(b) shows that there is only very little background just below the GT states. It shows furthermore that there has to be GT strength in the Q-value region -20 MeV $\geq Q \geq -30$ MeV which means that the GT strength indeed is extending beyond the main peak. This conclusion is quite definite. It will not be modified if we would use other strength distribution functions since the background being flat is quite insensitive to such a change. Comparing the calculated spectrum in Fig. 2(a) with the *background* cross section in Fig. 2(b), one notices that the extension of GT strength beyond the main peak actually follows in a very natural way from the line shape of the experimental GT resonance. With our assumption of minimal spreading the GT strength extends only up to $Q = -40$ MeV, which is a much smaller value than that derived from 2p2h configuration mixing calculations.[14,29–32]

The theoretical spectrum in Fig. 2(a) calculated with RPA slightly overestimates the experimental one in the Q-value range, 0 MeV $\geq Q \geq -40$ MeV. Considering this

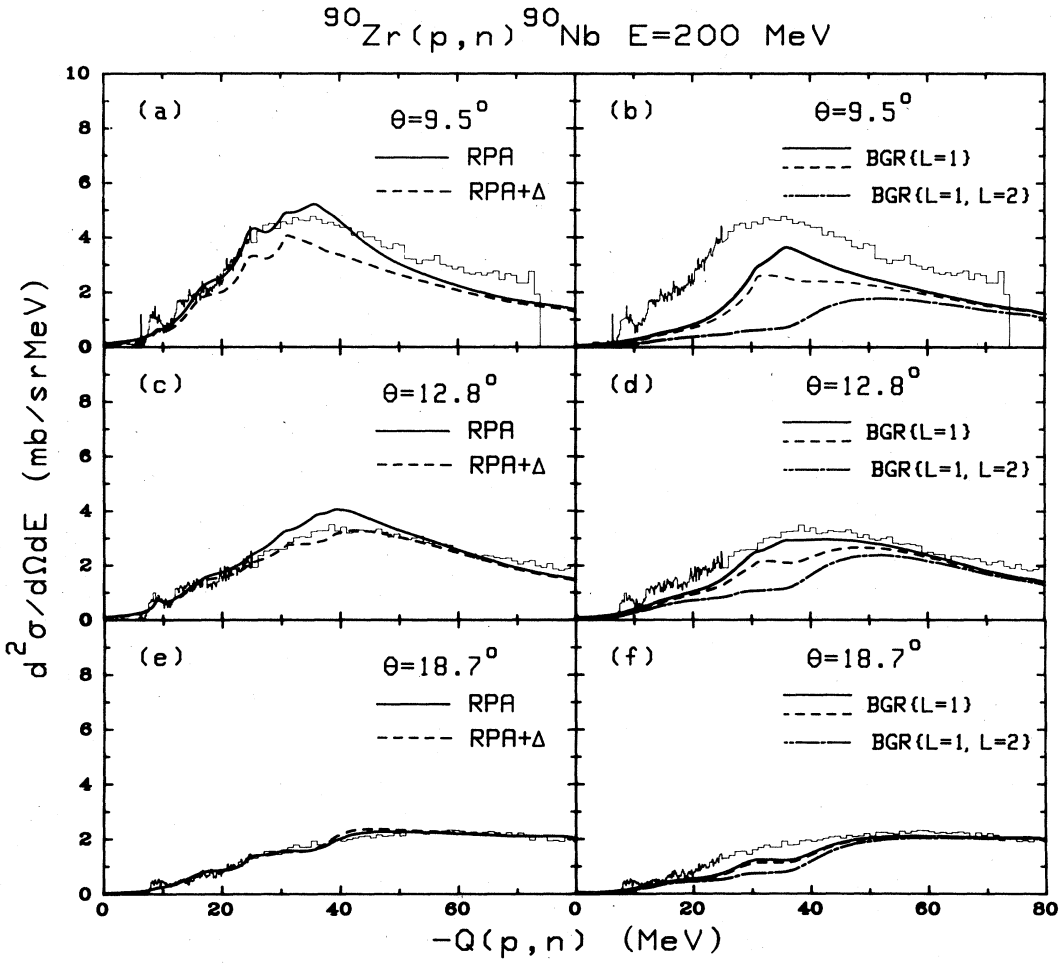

FIG. 3. Same as Fig. 2 but now for the scattering angles $\theta=9.5°$, 12.8°, and 18.7°. The full and dashed curves in (b), (d), and (f) represent the *background* (BGR) with respect to the $1\hbar\omega$, $L=1$ resonance (BGR $L=1$) calculated either with RPA (full line) or RPA + Δ (dashed line). Also the *background* with respect to the $1\hbar\omega$, $L=1$, *and* the $2\hbar\omega$, $J^\pi=1^+,2^+,3^+$ resonances calculated with RPA is shown (BGR $L=1,L=2$). By substracting the latter from the BGR $L=1$ cross section one obtains the strength distribution of the $2\hbar\omega$, $J^\pi=1^+,2^+,3^+$ states.

Q-value range we need a quenching of 15% of the theoretical spectrum in order to bring experiment and theory into agreement. Unfortunately we cannot decide whether this quenching should be due to the Δ isobar effect or due to additional spreading of both the GT strength and the $L=1$ and $L=2$ strength. A larger asymmetric spreading as required by 2p2h calculations would shift more strength to higher excitation energies. Such an additional shift would actually be welcome since the theory is underestimating the data at high negative Q values with the present widths.

We can, however, show that the Δ isobar effect cannot be very large, i.e., not 30% or 50% of the minimal sum rule limit $S_{\beta^-}=3(N-Z)$ as was required by several authors.[9] This can be seen from the dashed curve in Fig. 2(a) which is the result of a calculation performed with generalized RPA wave functions which include Δ isobar-nucleon hole components explicitly. The Δ isobar admixtures were adjusted such that the total B(GT) strength is quenched by 30%. This can be obtained by an appropriate adjustment of the $(\delta g_0')_{\Delta N}$ parameter in the ΔN^{-1} residual interaction. A value $(\delta g_0')_{\Delta N}=0.4(f^*/f)$ leads to such a 30% quenching of the total GT strength. Using the corresponding RPA + Δ wave functions in the cross section calculations we obtain the dashed curve in Fig. 2(a). In spreading the strength, the same widths were used as in the RPA result. The spectrum calculated with RPA + Δ underestimates the data everywhere and particularly strongly in the GT resonance region. Within the framework of our model (Sec. II) where we neglect 2p2h admixtures into the ground state of ^{90}Zr there is obviously no need for such a large Δ isobar-nucleon hole quenching. Actually we underestimate the experimental zero degree (p,n) cross section then by approximately 37 mb if we consider the whole Q-value range from 0 MeV $\geq Q \geq -70$ MeV. However, we also point out that the inclusion of ground state correlations of the 2p2h-type might modify this conclusion.[14]

B. The 4.5° spectrum and the $L=1$ resonance

In Fig. 2(c) we show the results for the 4.5° spectrum. At this angle the GT cross section is still large and the $L=1$ resonance has its peak cross section. The spectrum calculated with RPA (full curve) describes the data rather well although its magnitude is somewhat too large in the low Q value region (0 MeV $\geq Q \geq -40$ MeV) and too small at high negative Q values (-40 MeV $\geq Q \geq -70$ MeV). The spectrum calculated with a 30% Δ isobar effect (dashed curve), on the other hand, underestimates the data everywhere, in particular also in the GT and $L=1$ resonance region. Apparently, we have here a similar situation as for the 0° spectrum. A 30% quenching effect due to Δ isobars is too large. It is interesting that the RPA spectrum describes shape and magnitude of the $L=1$ resonance rather well while it overestimates the GT resonance region. The explanation for this can be found from Fig. 2(d) where we show the background with respect to the GT resonance [full curve (RPA), dashed curve (RPA + Δ)], and with respect to both the GT *and* $L=1$ resonances [dot-dashed curve (RPA), dot-dot-dashed curve (RPA + Δ)]. By subtracting the dot-dashed from the full curve we obtain the strength distribution of the $L=1$ resonance. Inspecting now the GT resonance region ($Q \sim -15$ MeV) we find that there is an appreciable background below the GT resonance which is due to the extension of the $L=1$ resonance to this low Q value. We remark that the distribution of $L=1$ strength is not necessarily as well determined by the RPA as that of the GT strength because of the more complicated unperturbed ph spectrum. Therefore, a slight redistribution of $L=1$ strength to higher excitation energies would immediately lead to an improved description of the 4.5 deg RPA spectrum. The same is true for the 0° spectrum where also a large part of the background just below the GT resonance is due to the $L=1$ strength, as can be seen from a comparison of the full and dot-dashed curves in Fig. 2(b).

The $L=1$ resonance is a superposition of three resonances with spin parities $J^\pi=0^-$, 1^-, and 2^-. In Figs. 4(a) and 4(b) we show their separate contributions to the cross section at angles of $\theta=4.5°$ and $\theta=9.5°$, respectively, where the $L=1$ resonance has its largest cross section. The 2^- states are lowest in excitation energy, then follow the 1^- states, and the 0^- states have the highest excitation energy. The sum of all these cross sections (full curve) forms a resonance shape which peaks around $Q=-24$ MeV and has a total width of about 15 MeV.

In Table I, the second, the third, and the fourth columns, we give the detailed numbers for the cross sections contributed by the individual J^π resonances to the total $L=1$ cross section at the different scattering angles θ. These cross sections include, besides the $1\hbar\omega$, also the $3\hbar\omega$ 0^-, 1^-, and 2^- transition strength. The 2^- cross sections are largest at all scattering angles but the 0^- and 1^- cross sections also give appreciable contributions.

C. The 9.5° spectrum and the $L=2$ resonance

In Fig. 3(a) we show the results for the 9.5° spectrum. At this angle the GT cross section contribution to the spectrum is negligibly small and the shape of the spectrum is dominantly determined by the $L=1$ and the $2\hbar\omega$ ($L=0$ and $L=2$) resonances. Again the theoretical spectrum calculated with RPA provides a good description of

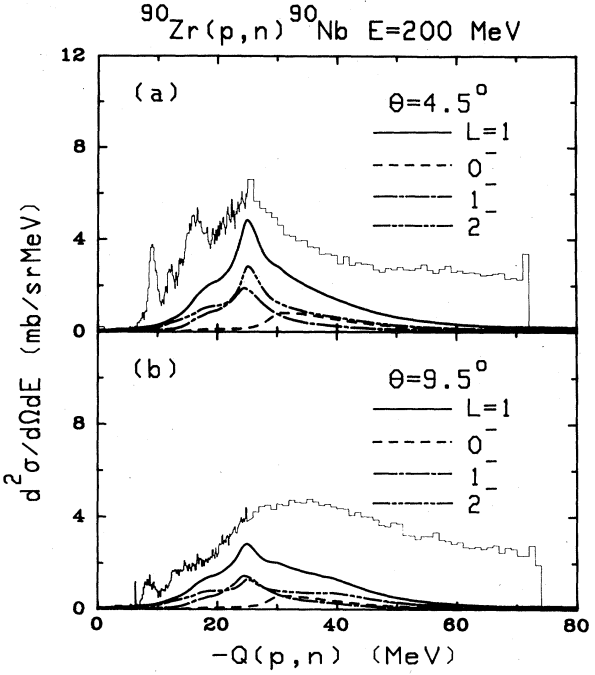

FIG. 4. The cross section contributions of the $1\hbar\omega$, $J^\pi=0^-,1^-,2^-$ states to the 4.5° (a) and 9.5° (b) spectra, respectively. These states form together the $L=1$ resonance. The theoretical cross sections were calculated with RPA wave functions. The full curve represents the sum of the 0^-, 1^-, and 2^- cross sections.

TABLE I. Energy integrated theoretical cross sections for various classes of final nucleus states. In the second to fifth columns, we list the individual cross sections to states which form the $1\hbar\omega$, $L=1$ resonance ($J^\pi=0^-,1^-,2^-$) and in the sixth to ninth columns we give analogous cross sections for the $2\hbar\omega$, $L=2$ resonance ($J^\pi=1^+,2^+,3^+$). The numbers listed were calculated with RPA wave functions or generalized RPA + Δ wave functions (numbers in parentheses).

$\theta_{c.m.}$	$L=1$ resonance			$L=2$ resonance		
	0^-	1^-	2^-	1^+	2^+	3^+
(deg)		(mb/sr)			(mb/sr)	
0.0	15	5	32	27	4	11
	(12)	(5)	(28)	(23)	(2)	(10)
4.5	17	25	43	29	8	15
	(14)	(23)	(30)	(20)	(5)	(14)
9.5	11	20	31	32	6	26
	(9)	(16)	(19)	(17)	(4)	(21)
12.8	4	7	22	17	2	20
	(3)	(5)	(19)	(7)	(1)	(16)
18.7	2	3	11	3	1	7
	(3)	(3)	(15)	(2)	(1)	(5)

the experimental data, while the spectrum calculated with RPA + Δ is too small in magnitude.

The $2\hbar\omega$ excitation with $L=0$ and $L=2$ consists of a superposition of three resonances with spin parities $J^\pi=1^+$, 2^+, and 3^+. In Figs. 5(a) and (b) we show their separate contributions to the 9.5° and 12.8° spectrum, respectively. It can be seen that the 3^+ resonance is very broad with the peak cross section at around $Q=-25$ MeV, while the 1^+ resonance has a smaller width and peaks at around $Q=-38$ MeV.

In Table I, the fifth to seventh columns, we list the numbers for the cross sections contributed by the individual J^π states to the $2\hbar\omega$ resonance at different scattering angles θ. The 1^+ states give a large contribution of 27 mb to the 0° cross section. This contribution should, however, not be mixed up with the GT strength which enters in the sum rule, Eq. (1), and which is connected with the β decay operators $\sigma\tau_\pm$. The expectation value of this operator with $2\hbar\omega$ configurations is zero because of the orthogonality of the radial wave functions. The $2\hbar\omega$ 1^+ strength is mainly excited with the operator $f(r)(Y_2\times\sigma)_{1^+}\tau_-$ which is part of the hadronic transition operator and which introduces a radial dependence.[28] Therefore, it is obvious that this cross section contribution should not be included in the sum rule of Eq. (1).

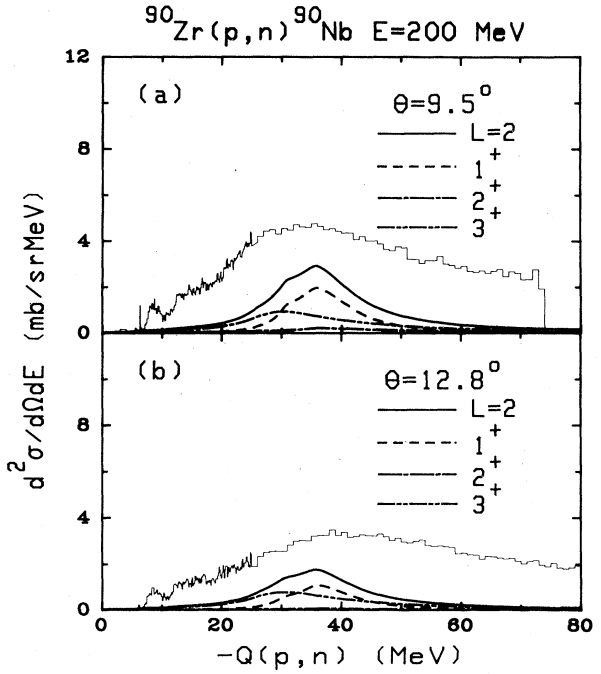

FIG. 5. The cross section contributions of the $2\hbar\omega$, $J^\pi=1^+,2^+,3^+$ states to the 9.5° (a) and 12.8° (b) spectra, respectively. These states form together the $L=2$ resonance. The theoretical cross sections were calculated with RPA wave functions. The full curve represents the sum of the 1^+, 2^+, and 3^+ cross sections.

D. The 12.8° and the 18.7° spectra

Particularly important for our discussions are the results for the high angle spectra at $\theta=12.8°$ and $\theta=18.7°$ which are shown in the lower part of Fig. 3. At these scattering angles both the GTR and the $L=1$ resonance give a comparatively small contribution to the total (p,n) spectrum (see Tables I and III). The shape and magnitude of these spectra are therefore mainly determined by states of other multipolarities.

In Figs. 3(c) and (e) we compare the calculated 12.8° and 18.7° spectra to the data. The full curve again denotes the result obtained with RPA, and the dashed curve denotes the one obtained with RPA + Δ. While the RPA result overestimates the data somewhat in the 12.8° spectrum, it produces, on the other hand, a perfect description of the 18.7° spectrum. One reason for the overestimation in the 12.8° spectrum is that the 3^- and 4^- states which are treated in our calculations as unperturbed ph states, i.e., without RPA correlations, have their peak cross section at this angle. The inclusion of RPA correlations would therefore lead to a reduction in cross section. The contribution of the $L=2$ resonance is still appreciable at this angle as can be seen from Fig. 3(d) where we show the background cross section with respect to the $L=1$ resonance (full curve) and with respect to the $L=1$ *and* $L=2$ resonances (dot-dashed curve). The same is shown for the 18.7° spectrum in Fig. 3(f).

E. Convergence of the cross section calculation

The good description of the small and large angle scattering data by our model calculations leads us to the following important conclusion: At 200 MeV incident energy the whole (p,n) spectra up to $E_x=70$ MeV are still a result of one-step processes only. Two-step processes with explicit excitation of 2p2h states are still suppressed. This conclusion has important consequences for the interpretation of the forward angle ($\theta=0°$, 4.5°, and 9.5°) spectra. It implies that the experimental cross section area at large negative Q values in Figs. 2 and 3, which is not yet described by our calculations, should also be the result of one-step processes. This is, however, only possible if there exists additional 1p1h transition strength in the high Q-value region $-40\text{ MeV}\geq Q\geq -70$ MeV which produces forward peaked angular distributions, i.e., the latter have to be of $L=0$, $L=1$, or $L=2$ shape. All strength of this type, however, is already included in our calculations, but it is dominantly located in the low excitation energy region where it actually leads to too large theoretical cross sections. A simple and consistent solution to this problem can be obtained if we assume an even stronger spreading of the $L=0$, $L=1$, and $L=2$ strength to higher excitation energies than we have done so far. With this assumption the overestimate of the data by the theory at low excitation energies and small angles and the underestimate at high excitation energies would disappear, while the results for the large angle spectra remain essentially unchanged.

The preceding conclusion could only be modified if there would exist a special class of two-step processes which would produce strongly forward peaked angular

distributions. One condition for a cross section to be large at 0° is that the total angular momentum transfer **L** in the scattering process has to be small, preferentially $\mathbf{L}=0$. In the case of a two-step process the total angular momentum transfer **L** is the sum of the angular momenta transferred in each step: $\mathbf{L}=\mathbf{L}_1+\mathbf{L}_2$, where $\mathbf{L}_1$ is the angular momentum transferred in the first step and $\mathbf{L}_2$ is the one transferred in the second step. Since we require $\mathbf{L}=0$, we have $\mathbf{L}_1=-\mathbf{L}_2$. A further condition for a two-step cross section being large is that it must be composed of two strong transitions, each of which has to possess a reasonably large form factor. The most important processes will be inelastic excitation of the target nucleus followed by charge exchange or vice versa. This follows from the fact that one needs a strong projectile-target nucleus coupling in each step in order to obtain a large form factor. The strong central force components at intermediate energies are the spin-isospin independent component V_0 and the spin-isospin flip producing component $V_{\sigma\tau}$.[21] One possibility, for instance, which fulfills all the conditions required is the inelastic excitation of the giant monopole resonance followed by a GT transition or vice versa. Since the giant monopole resonance occurs in ^{90}Zr at $E_x=16$ MeV (Ref. 33), the Q value for this two-step process will amount roughly to $Q=-35$ MeV. While the described process consists of a $2\hbar\omega$ excitation followed by a $0\hbar\omega$ charge exchange transition, one can also imagine a $1\hbar\omega$ inelastic excitation of an $L=1$ type (excitation of the giant dipole resonance) followed by a $1\hbar\omega$ $L=1$ charge exchange mode. Such a two-step process would contribute to the 0° cross section at around $Q=-40$ MeV. So, altogether one could expect that two-step contributions could become important for Q values beyond $Q=-35$ MeV. Therefore, we have calculated such types of processes using an extended version[34] of the computer code FROST-MARS which can perform a completely antisymmetric, second-order DWBA calculation. We found that the cross sections due to such two-step processes are smaller than the first-order ones by more than three orders of magnitude (of the order 10^{-3} mb/sr at 0°). Although the density of the 2p2h states becomes large at high excitation energies, it seems nevertheless unlikely to us that the explicit excitation of 2p2h states can give large contributions to the cross section since the two-step cross sections which we expected to be strongest are already so small.

F. Quenching due to the Δ isobar effect

In view of the problems concerning the spreading of GT strength (and those of other resonances) due to the 2p2h configuration mixing effect, it seems to be advisable for a careful discussion of the Δ isobar quenching effect to work with energy integrated cross sections. In Table II we list the energy integrated experimental cross sections (second column) and the calculated ones (third column) as a function of the scattering angle θ. The integration interval extends from zero to $Q=-70$ MeV. The theoretical cross sections were calculated either with RPA or RPA + Δ (numbers in parentheses). The RPA result reproduces the measured cross sections at all scattering angles within an accuracy of 10%, while the cross sections calculated with RPA + Δ underestimate the corresponding experimental values at forward angles ($\theta=0°$, 4.5°, and 9.5°) by about 20% to 25%. At $\theta=18.7°$ the cross sections based on RPA and RPA + Δ are essentially the same and agree with experiment. From the results in Table II one might be tempted to conclude that there should be *no* quenching due to Δ isobars. This conclusion is, however, daring since we have so far not included the following important effect in our analysis of the data. Bertsch and Hamamoto[14] have pointed out that by shifting strength from the low to the high excitation energy region one simultaneously creates *new* strength at low excitation energies. This is due to the fact that a strong spreading of the 1p1h strength due to the admixture of 2p2h configurations also implies the presence of strong 2p2h correlations in the target nucleus ground state. From the point of view of perturbation theory both processes are of the same order in the residual ph interaction. The presence of strong ground state correlations, on the other hand, gives the possibility to create new S_{β_-} and S_{β_+} strength which have to be equal in magnitude in order to fulfill the sum rule in Eq. (1). How much new strength is really created depends sensitively on the interference of the ground state correlations with the final state correlations. This interference is a coherent process making an estimate of the created strength rather difficult. From an experimental point of view this question can only be answered by performing (n,p) experiments at the same target nucleus which would measure the S_{β_+} strength directly. In lack of such (n,p) experiments one can also get a good estimate on the amount of S_{β_+} (S_{β_-}) strength to be expected from ground state correlations by considering the (p,n) reactions from spin saturated $N=Z$ nuclei like ^{16}O or ^{40}Ca. In the independent particle model these nuclei have zero GT strength. In the presence of ground state correlations the S_{β_-} strength becomes unequal to zero (but equally large to the S_{β_+} strength) and should reflect itself in an enhanced zero degree (p,n) cross section. We have performed a preliminary calculation for the reaction ^{40}Ca(p,n) and found that as much as 15 mb of the zero degree 200 MeV ^{40}Ca(p,n) cross section might be due to GT strength. This value is in good agreement with

TABLE II. Energy integrated experimental and theoretical cross sections for different scattering angles θ. The theoretical cross sections were calculated either with RPA wave functions or generalized RPA + Δ wave functions (numbers in parentheses). All numbers are subject to ~10% uncertainty due to the choice of optical potential parameters.

$\theta_{c.m.}$ (deg)	σ_{exp} 0 MeV ≥ Q ≥ −70 MeV (mb/sr)	σ_{cal} 0 MeV ≥ Q ≥ −70 MeV (mb/sr)
0.0	215	232 (178)
4.5	212	211 (164)
9.5	203	192 (156)
12.8	150	164 (144)
18.7	102	102 (104)

results[31] obtained from explicit 2p2h calculations.

In view of these problems we are led to draw the following conclusions with respect to the Δ isobar quenching effect: Quenching due to Δ isobars is only needed in order to explain the 0° ^{90}Zr(p,n) spectrum if there exists a large amount of S_{β_+} strength in ^{90}Zr. Otherwise, the (p,n) cross sections are compatible with the strength predictions as obtained from the usual RPA. The strength has to be spread out, however, over a relatively large energy range. In Table III, second column, we list the calculated total GT cross section as a function of scattering angle θ and in the third column the corresponding fraction of GT cross section which is situated in the high energy tail (-20 MeV $\geq Q \geq -70$ MeV) of the (p,n) spectrum. The latter amounts to 20–25 % of the total GT strength. Note also that at small scattering angles (q transfers) the RPA + Δ GT cross section is smaller than the one obtained with RPA, while this behavior is reversed at high scattering angles as it should. At large momentum transfers the Δ isobar effect leads to an enhancement of the GT cross section[36] instead of a quenching.

G. Strength distribution estimates from the experimental spectra

After the analysis of the complete forward angle (p,n) spectra where we also obtained the angular dependence of the different modes, one can make simple estimates for the strength distribution of the various multipoles using the experimental data only. In the following we want to demonstrate this. Let us start with the large angle scattering data. As the $L=2$ resonance cross sections peak at 9.5° and the $L=0$ and $L=1$ resonance cross sections are small at 18.7°, we can determine the $L=2$ strength distribution by subtracting the experimental 18.7° spectrum from the data at 9.5°. This procedure is particularly safe for large Q values, $Q \leq -40$ MeV, since the cross section at this high Q value and at large scattering angles is produced by $L=3$ and $L=4$ transitions whose angular distributions are still rising going from $\theta=9.5°$ to 18.7°. By this subtraction method one finds that the $L=2$ strength extends at least up to $Q=-50$ MeV. Similarly we can subtract the high energy tail of the $\theta=0°$ spectrum from the $\theta=4.5°$ spectrum. Since the $L=1$ cross section is growing from 0° to 4.5° we can determine up to which Q value we should expect at least $L=1$ strength. We find $Q=-40$ MeV for $L=1$. Finally, we subtract the experimental 12.8° spectrum from the 0° spectrum. At 12.8° the GT cross section is approximately zero and the $L=1$ cross section is small. Therefore, by subtracting the 12.8° spectrum from the 0° spectrum, we obtain a lower limit for the spread of GT strength. We find that the GT strength should at least be spread out up to $Q=-35$ MeV. If we compare these experimental limits for the energy spread of the different charge exchange modes with those which we require from our analysis of the (p,n) spectra, we find that they essentially agree. This gives us further confidence in our conclusion that a large part of the $L=0$, $L=1$, and $L=2$ strength is residing in the high energy tail of the ^{90}Zr(p,n) spectrum.

TABLE III. Total calculated GT cross sections for different scattering angles θ. In the third column, we list the GT cross section residing in the high energy tail of the theoretical spectrum.

$\theta_{c.m.}$ (deg)	σ_{GT} 0 MeV $\geq Q \geq -70$ MeV (mb/sr)	σ_{GT} -20 MeV $\geq Q \geq -70$ MeV (mb/sr)
0.0	115(76)	25 (17)
4.5	45(29)	9 (6)
9.5	5 (6)	1 (1)
12.8	1 (4)	0 (1)
18.7	1 (1)	0 (0)

H. Comparison with other calculations

Nuclear structure calculations (see Ref. 29 for a recent review) have been performed for electric giant resonances which consider the spreading of these states due to their coupling to 2p2h configurations. Recently, several groups[30–32] have carried out similar studies for the GT states. We refer here to a 2p2h calculation for the GT strength distribution in ^{90}Zr as performed by Cha *et al.*[32] These authors find that the GT strength function in ^{90}Zr exhibits a long tail which extends up to 60 MeV excitation energy. The tail includes as much as 25% of the total GT strength. Similar results have also been obtained by other groups.[14,30–32,35] All these calculations agree qualitatively with our present result.

IV. SUMMARY AND CONCLUSIONS

We have presented a microscopic analysis of forward angle ^{90}Zr(p,n) spectra at an incident energy of $E_p=200$ MeV. The analysis shows that the whole spectra up to excitation energies of $E_x=70$ MeV are the result of direct one-step processes only and that the spectra can be regarded as the linear $\sigma\tau$ response of the target nucleus to the probing (p,n) field. The spectra are *background*-free with the understanding that *background* stands for a cross section which is produced by complicated multistep processes. Both the peaks and the continuous parts of the spectra are due to 1p1h excitations of the target nucleus. Therefore, one can decompose the spectra into the various multipoles and obtain in this way information on the strength distribution of final nuclear states with different J^π.

Two different analyses of the ^{90}Zr(p,n) spectra have been performed in this paper. One has been carried out with common RPA wave functions and the other with generalized RPA wave functions which include Δ isobar degrees of freedom. We find that the theoretical spectra calculated with RPA describe the experimental data at all scattering angles rather well, while the spectra obtained with RPA + Δ underestimates them at forward angles. From this result, we deduce that the measured (p,n) cross sections are compatible with the transition strength predictions as obtained from the RPA.

Concerning the quenching of the total GT strength, our calculations suggest that the amount of GT strength in the low excitation energy region can be as large as the

lower sum rule limit, i.e., $S_{\beta_-}=3(N-Z)$, without leading to contradiction with the present (p,n) data. Quenching due to Δ isobars is only needed if $S_{\beta_+}\neq 0$. This is the case as soon as there exist 2p2h or other correlations in the ground state of ^{90}Zr which are not included in the RPA. From the sum rule $S_{\beta_-}=3(N-Z)+S_{\beta_+}$ we see that $S_{\beta_+}\neq 0$ implies also the production of additional S_{β_-} strength. From our analysis of the data, we cannot afford more S_{β_-} strength than $3(N-Z)$. Therefore any additional S_{β_-} strength has to be quenched away, for instance, by the Δ isobar quenching mechanism. How much S_{β_+} strength is present in ^{90}Zr can be determined from a ^{90}Zr(n,p) experiment. Therefore, (n,p) experiments are very crucial tools to settling the problem on the role of the Δ isobar in nuclei.

The authors want to thank C. Gaarde, S. Krewald, V. A. Madsen, K. Nakayama, T. Udagawa, and J. Wambach for very stimulating discussions.

*Also at Institut für Theoretische Kernphysik, Universität Bonn, D-5300 Bonn, Federal Republic of Germany.

[1]R. R. Doering, A. Galonsky, D. Patterson, and G. F. Bertsch, Phys. Rev. Lett. **35**, 1961 (1975).

[2]D. E. Bainum, J. Rapaport, C. D. Goodman, D. J. Horen, C. C. Foster, M. B. Greenfield, and C. A. Goulding, Phys. Rev. Lett. **44**, 1751 (1980).

[3]C. D. Goodman, C. A. Goulding, M. B. Greenfield, J. Rapaport, D. E. Bainum, C. C. Foster, W. G. Love, and F. Petrovich, Phys. Rev. Lett. **44**, 1755 (1980).

[4]D. J. Horen, C. D. Goodman, C. C. Foster, C. A. Goulding, M. G. Greenfield, J. Rapaport, E. Sugarbaker, T. G. Masterson, F. Petrovich, and W. G. Love, Phys. Lett. **95B**, 27 (1980); D. J. Horen, C. D. Goodman, D. E. Bainum, C. C. Foster, C. Gaarde, C. A. Goulding, M. B. Greenfield, J. Rapaport, T. N. Taddeucci, E. Sugarbaker, T. Masterson, S. M. Austin, A. Galonsky, and W. Sterrenburg, *ibid.* **99B**, 383 (1981).

[5]C. Gaarde, J. Rapaport, T. N. Taddeucci, C. D. Goodman, C. C. Foster, D. E. Bainum, C. A. Goulding, M. G. Greenfield, D. J. Horen, and E. Sugarbaker, Nucl. Phys. **A369**, 258 (1981).

[6]K. I. Ikeda, S. Fujii, and J. I. Fujita, Phys. Lett. **3**, 271 (1963).

[7]S. Krewald, F. Osterfeld, J. Speth, and G. E. Brown, Phys. Rev. Lett. **46**, 103 (1981); G. F. Bertsch, D. Cha, and H. Toki, Phys. Rev. C **24**, 533 (1981).

[8]C. Gaarde, Nucl. Phys. **A396**, 127c (1983); J. Rapaport, in *The Interaction Between Medium Energy Nucleons in Nuclei—1982,* Proceedings of the Workshop on the Interaction Between Medium Energy Nucleons in Nuclei (Indiana University Cyclotron Facility), AIP Conf. Proc. No. 97, edited by H. O. Meyer (AIP, New York, 1983), p. 365.

[9]M. Ericson, A. Figureau, and C. Thevenet, Phys. Lett. **45B**, 19 (1973); M. Rho, Nucl. Phys. **A231**, 493 (1974); K. Ohta and M. Wakamatsu, *ibid.* **A234**, 445 (1974); J. Delorme, M. Ericson, A. Figureau, and C. Thevenet, Ann. Phys. (N.Y.) **102**, 273 (1976); E. Oset and M. Rho, Phys. Rev. Lett. **42**, 42 (1979); W. Knüpfer, M. Dillig, and A. Richter, Phys. Lett. **95B**, 349 (1980); A. Härting, W. Weise, H. Toki, and A. Richter, *ibid.* **104B**, 261 (1981); H. Toki and W. Weise, *ibid.* **97B**, 12 (1980); A. Bohr and B. R. Mottelson, *ibid.* **100B**, 10 (1981); G. E. Brown and M. Rho, Nucl. Phys. **A327**, 397 (1981); H. Sagawa and Nguyen van Giai, Phys. Lett. **118B**, 167 (1982).

[10]T. Suzuki, S. Krewald, and J. Speth, Phys. Lett. **107B**, 9 (1981).

[11]F. Osterfeld, S. Krewald, J. Speth, and T. Suzuki, Phys. Rev. Lett. **49**, 11 (1982); T. Izumoto, Nucl. Phys. **A395**, 189 (1983).

[12]I. S. Towner and F. C. Khanna, Phys. Rev. Lett. **42**, 51 (1979).

[13]A. Arima and H. Hyuga, in *Mesons in Nuclei,* edited by D. Wilkinson (North-Holland, Amsterdam, 1979), p. 683; K. Shimizu, M. Ichimura, and A. Arima, Nucl. Phys. **A226**, 282 (1978); A. Arima in *Spin Excitations in Nuclei,* edited by F. Petrovich, G. E. Brown, G. T. Garvey, C. D. Goodman, R. A. Lindgran, and W. G. Love (Plenum, New York, 1984).

[14]G. F. Bertsch and I. Hamamoto, Phys. Rev. C **26**, 1323 (1982).

[15]F. Osterfeld, Phys. Rev. C **26**, 762 (1982); F. Osterfeld in *Spin Excitations in Nuclei,* edited by F. Petrovich, G. E. Brown, G. T. Garvey, C. D. Goodman, R. A. Lindgran, and W. G. Love (Plenum, New York, 1984).

[16]F. Osterfeld and A. Schulte, Phys. Lett. **138B**, 23 (1984); F. Osterfeld and A. Schulte, in *Highly Excited States and Nuclear Structure,* edited by N. Marty and Nguyen van Giai, J. Phys. **45**, 13 (1984).

[17]F. Osterfeld, S. Krewald, H. Dermawan, and J. Speth, Phys. Lett. **105B**, 257 (1981).

[18]K. Ikeda, Prog. Theor. Phys. **31**, 434 (1964).

[19]H. C. Chiang and J. Hüfner, Nucl. Phys. **A349**, 466 (1980).

[20]A. K. Kerman, H. McManus, and R. M. Thaler, Ann. Phys. (N.Y.) **8**, 551 (1959).

[21]W. G. Love and M. A. Franey, Phys. Rev. C **24**, 1073 (1981).

[22]G. F. Chew and F. E. Low, Phys. Rev. **101**, 1570 (1956).

[23]F. Osterfeld, FROST-MARS code (unpublished).

[24]C. Gaarde, private communication.

[25]A. Nadasen, P. Schwandt, P. P. Singh, W. W. Jacobs, A. D. Bacher, P. T. Debevec, M. D. Kaitchuck, and J. T. Meek, Phys. Rev. C **23**, 1023 (1981).

[26]G. M. Crawley *et al.,* Phys. Rev. C **26**, 87 (1982).

[27]G. R. Satchler, Nucl. Phys. **A394**, 189 (1983).

[28]F. Osterfeld, J. Wambach, H. Lenske, and J. Speth, Nucl. Phys. **A318**, 45 (1979).

[29]G. F. Bertsch, P. F. Bortignon, and R. A. Broglia, Rev. Mod. Phys. **55**, 287 (1983).

[30]J. Wambach and B. Schwesinger, in *Highly Excited States and Nuclear Structure,* edited by N. Marty and Nguyen van Giai, J. Phys. **45**, 281 (1984); V. G. Sloviev, *ibid.* **45**, 69 (1984); W. Knüpfer, *ibid.* **45**, 513 (1984).

[31]P. F. Bortignon, R. A. Broglia, and Xia Ke-Ding, see Ref. 30, p. 209.

[32]D. Cha, B. Schwesinger, J. Wambach, and J. Speth, Nucl. Phys. **A430**, 321 (1984).

[33]D. H. Youngblood, J. M. Moss, C. M. Rozsa, J. D. Bronson, A. D. Bacher, and D. R. Brown, Phys. Rev. C **13**, 994 (1976).

[34]F. Osterfeld, J. Wambach, and V. A. Madsen, Phys. Rev. C **23**, 179 (1981).

[35]I. S. Towner and F. C. Khanna, Nucl. Phys. **A399**, 334 (1983).

[36]F. Osterfeld, T. Suzuki, and J. Speth, Phys. Lett. **99B**, 75 (1981).